

IXRF Optimization for Harmful Element Detection in Iranian Dust

H.R. Mansourbahmani, A. Negarestani¹ and M.R. Rezaie^{1*}

Department of Photonics, Kerman Graduate University of Advanced Technology, P.O. Box 76315–117, Mahan, Iran

¹Department of Nuclear Engineering, Kerman Graduate University of Advanced Technology

P.O. Box 76315–117, Mahan, Iran

✉ mr.rezaie@kgut.ac.ir

Received September 15, 2017; revised and accepted February 19, 2018

Abstract: Detection of hazardous and radioactive (HR) elements in dust is very important for environment and human health. About 70 percent of Iran's climate is arid and semi-arid, and one of the environmental challenges that it faces includes approaching dust storms from the southern and the western countries that neighbour Iran. Therefore, to solve this problem, it seems necessary to make a portable device to detect the HR elements of dust to eliminate social anxiety. In the present study, an isotopic X-ray fluorescence (IXRF) device was optimized to identify HR elements in dust, which arrive as environmental pollutants from neighbouring countries situated to the west and the south of Iran. Simulation results have indicated that the elements could be recognized by an IXRF device after the combination of ²⁴¹Am (26.4 and 59.6 keV) and ⁵⁷Co (122 keV) as the source. In this device, a scintillation detector was used for the X-ray spectroscopy of elements. If the CsI(Tl) detector that shielded with 1 mm copper, aluminum and tungsten, then the IXRF device with 1.64 mCi ²⁴¹Am and ⁵⁷Co mixed source is able to measure the HR elements with low of detection (LOD) about 10 ppm. Therefore, the optimized IXRF device can be introduced to detect the HR elements in dust.

Key words: Dust elements, IXRF device, Hazardous, LOD, Radioactive, MCNPX.

Introduction

Detection of HR elements in dust is environmentally important because it can have detrimental effects on the health of a society (Župunski et al., 2010; Plumejeaud et al., 2010; Kampa and Castanas, 2008; Genc et al., 2012; Briner, 2010; Pirsaeheb et al., 2014). In this regard, various chemical and physical methods have been used. One of the most important chemical methods is atomic absorption spectrometry (Tonetti and Innocenti, 2009; Gondal et al., 2010). The physical methods mainly include the techniques of laser-induced breakdown spectroscopy (LIBS) and energy dispersive X-ray fluorescence (ED-XRF) (Genc et al., 2012; Yu et al., 2002), which is a rapid and non-destructive method.

Certain radioactive elements have a specific range of gamma rays, which can be used as an X-ray source instead of an X-ray tube in the ED-XRF technique. Today, the various radioactive sources such as ⁵⁷Co, ⁶⁰Co, ¹³⁷Cs, ⁵⁵Fe and ²⁴¹Am, are used in this regard (Zarasvandi et al., 2011). Each radioactive source has the ability to identify a few of the elements within a specific range. The aim of this study is to detect elements in the wide range of $16 < Z < 92$.

To this end, a combination of several radioactive sources was used to detect HR elements in dust to the south and the west of Iran. In addition, the combination was aimed to increase the possibility of using two ²⁴¹Am (26.4 and 59.6 keV) and ⁵⁷Co (122 keV) mixtures as radioactive sources in an isotopic X-ray fluorescence

*Corresponding Author

(IXRF) technique based on Monte Carlo simulation to detect HR elements in dust as an environmental pollution factor.

Materials and Methods

The aim of the study was to assess the feasibility of detecting HR elements in the dust using the Monte Carlo method. Dust is a combination of different elements in the range of $16 \leq Z \leq 92$ and its pollutants and hazardous components are within the wide range of $24 < Z < 92$. In addition to normal elements, HR elements are brought to Iran by dust storms from the western and southern neighbouring countries (Zarasvandi et al., 2011). In this regard, some of the hazardous elements reported in the dust include Cr, Co, Ni, Cu, Zn, Zr, Nb, Mo and Pb. In dust samples, the presence of radioactive elements, such as U and Th (Table 1) (Zarasvandi et al., 2011), has been reported.

Each of these elements has its own characteristic X-ray spectrum, which is the special characteristic of each element. This spectrum is produced due to the transfer of electron from higher atomic layers to a vacant place in inner layers and its electrons inject out by X-ray irradiation.

The injection of electron could be from the K, L or M layer; therefore, the corresponding radiation is given the same name. The energy emitted from the K_{α} layer of HR elements in dust was calculated by Bearden and Burr (1967). According to Bearden and Burr data, the maximum energy emitted from the K_{α} layer of those elements was 98.43 keV. Therefore, a 100–120 KV X-ray tube was required for the accurate detection of various elements because of the extent of the characteristic X-ray energy spectrum of HR elements, leading to an increase in the size of the device and its higher costs and non-portability. Therefore, radioactive sources were used to eliminate this problem (Bamford et al., 2004; Greaves et al., 1997).

In this research, a combination of several radioactive sources with specific activities as an X-ray source was used in the IXRF device to determine HR elements in dust entering from neighbouring countries to the west and south of Iran. From the reported dust samples in the south and west of Iran, the AB1-87 pollutant sample was selected for simulation (Table 1) (Zarasvandi et al., 2011).

To optimize the IXRF device, the MCNPX code was used based on the Monte Carlo method. This code can trace the characteristic X-ray spectrum produced by the irradiation target. In the first stage, the gamma radiation of ^{241}Am (26.4, 59.6 keV) and ^{57}Co (122 keV) sources were separately radiated by HR elements in dust with their percentage.

In the second stage, a mixed radioactive source was created by combining ^{241}Am (26.4, 59.6 keV) and ^{57}Co (122 keV) sources and the dust sample was irradiated with it. The X-ray energy spectrum of the characteristic emission could be obtained using Tally *f8 in the input file for each step in the MCNP code. The input file of the MXNPX code is described in the following section to calculate the characteristic X-ray spectrum as a function of energy. At first, a view of the geometry defined in the input file is presented in Figure 1.

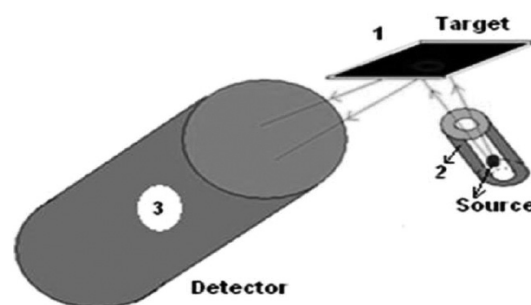


Figure 1: Schematic representation of IXRF system.

Table 1: The major and trace elements in the AB1-87 dust sample (Zarasvandi et al., 2011)

Trace elements	Elements	S	Cr	Co	Cl	Cu	Nb	Ni	Pb	Rb	Sr
	Percent	0.002	0.002	0.002	0.126	0.002	0.130	0.002	0.002	0.002	0.002
	Elements	W	Zr	Br	Zn	Mo	U	Th	Y		
	Percent	0.002	0.002	0.385	0.002	0.228	0.332	0.002	0.002		
Major elements	Elements	SiO ₂	Al ₂ O ₃	Fe ₂ O ₃	CaO	Na ₂ O	MgO	K ₂ O	TiO ₂	MnO	P ₂ O ₅
	Percent	6.8	6.2	0.34	1.62	4.2	2.1	28.6	0.067	0.01	0.26

In Figure 1, the cell number one is the target (or sample) and cell number two is a cylindrical tungsten shield, which is surrounded by an aluminum panel and contains ^{241}Am with energies of $E\gamma = 59.6$ (36%) and 26.4 (2.4%) (keV) or ^{57}Co sources with energies of $E\gamma = 122$ (85.6%), 14.4 (9.16%), and 136.47 (10.68%) (keV), or a mix of them. The cell number three is a cylindrical detector with a diameter of 3.83 cm, containing a crystal scintillator of CsI(Tl) , with a diameter of 3.81 cm and a height of 5.58 cm (Akkurt et al., 2015).

The target is irradiated with X-ray emitted from source. After the interaction of X-ray photons with the target atoms, the X-ray fluorescence is emitted by the target. The X-ray fluorescence spectrum reaches the inner surface of the cylindrical shell after radiation. In addition, Tally *f8 calculates the characteristic X-ray energy spectrum in the detector. The number of photons in the simulation was about 10^8 for reaching an error percentage of less than 1%. The percentage of HR elements in the AB1-87 dust sample is shown in Table 1 (Zarasvandi et al., 2011). In the Monte Carlo simulation to extract results related to the characteristic X-ray spectrum, the atomic number, mass number, and density of each element were required.

Results

Two stages are involved in the detection of HR elements in dust using the IXRF device: In the first stage, it is necessary to assess the validity of device performance, and, in the second stage, its components should be optimized after verifying the device.

First Stage: Assessing the Accuracy of IXRF Device

In this research, radioactivity sources have been used in order to eliminate the HV device and to shrink the IXRF device. The photons generated by the radioactive sources collide with the target and induce its elements to radiate X-ray fluorescence characteristics. If the target is any of the HR elements, then their characteristic X-rays have their own energy and pulse height. The elements of $Z < 42$ and $Z > 82$ irradiate with emitted photons from ^{241}Am and ^{57}Co sources respectively, and energy and pulse height are calculated with an output command called Tally.

In the MCNPX code, Tally is a command to calculate the dose, flux, energy, pulse height, etc., on a surface or within a volume. The most suitable Tallies for doing these calculations are *f8 and f8 Tallies respectively for calculating the energy remaining in the detector due

to the arrival of fluorescence radiation and the pulse height generated by it in the detector. Therefore, the fluorescence energy of the HR elements in the dust irradiated by ^{241}Am and ^{57}Co sources are obtained using *F8 Tally.

The results, compared with the experimental results, are shown in Table 2. The second column of this table presents the elements of HR in the dust, and the third and fourth columns show the e characteristic energy (K_α) of these elements obtained from an experiment (Thompson et al., 2016) and simulation with the IXRF device. The fifth column shows the percentage of relative error between experimental values and the simulation. The percentage of the relative error is equal to the ratio of the difference between the experimental values (exp) and the simulation (obs) to the experimental value as: Relative error = $(\text{exp} - \text{obs})/\text{exp} \times 100$.

The last column in Table 2 presents the values of $(\text{Exp} - \text{Obs})^2/\text{Exp}$ for each of the elements. The Pearson Chi-Square is obtained by their summation ($\chi^2 = \sum((\text{Exp} - \text{Obs})/\text{Exp})$). The Chi-Square is an appropriate parameter for calculating the degree of confidence. The degree of confidence can be calculated by critical values of Chi-Square and the degree of freedom (Coleman and Steele, 2009). The degree of freedom (df) is one less than the number of variables. According to Table 2, the df value is 10.

The results of Table 2 show that the percentage of errors in simulation and practical K_α energy for detecting of the HR elements in dust using the IXRF device varies from 0.06 to 0.52. The value of Pearson Chi-Square was $6.77\text{E-}3$ for detecting these elements using the IXRF device. According to critical values of Chi-Square and the degrees of freedom, the p -value is less than 0.01. Therefore, the confidence level for detecting the dust elements is more than 99%.

The low relative error and the p -value indicate the accuracy of the simulation. Therefore, the second stage of simulation can be started with a confidence more than 99%.

Second Step: Optimizing the IXRF Device

The second stage of the simulation is the optimization of the IXRF device for the detection of HR elements. Figure 1 gives an overview of the IXRF device. Optimization includes the main parameters of the device, such as the distance from the source to the sample, the distance from the sample to the detector, the X-ray angle with the sample surface, the angle of the detector to the sample, and the shielding of the source and the detector. The loss and absorption of radiation

Table 2: The Chi-Square for the calculation of the K_{α} energy of HR elements by the Monte Carlo Simulation

Classification	Element	$K_{\alpha}(keV)$			
		Experimental (Exp)	Simulation (Obs)	Percentage error	$(Exp - Obs)^2/Exp$
Hazardous elements	Cr	5.41	5.40	0.18	1.85E-5
	Co	6.93	6.90	0.43	1.30E-4
	Ni	7.48	7.45	0.40	1.20E-5
	Cu	8.04	8.05	0.12	1.24E-5
	Zn	8.64	8.60	0.46	1.85E-4
	Zr	15.77	15.75	0.12	2.53E-5
	Nb	16.61	16.60	0.06	6.02E-6
	Mo	17.48	17.45	0.17	5.15E-5
Radioactive elements	Pb	74.98	75.30	0.42	1.30E-3
	Th	93.35	93.80	0.48	2.17E-3
	U	98.43	98.95	0.52	2.75E-3
Pearson Chi-Square: $\chi^2 = \sum((Exp - Obs)^2/Exp) = 6.77E-3$					

emitted by the source and the sample are a function of distance.

The distances between the source and the sample and sample and the detector should be as low as possible. The results indicate that this distance depends on the source and the detector shield materials. When lead or tungsten is used as shield, these distances are minimized. The results of the calculation of the pulse height indicate that the fluorescence radiation intensity is the maximum if the radiation angle to the sample surface is 27 degrees. Owing to the high surface of the detector, its angle of exposure is not significantly affected by the energy absorbed by the detector. Moreover, due to the importance of shielding in the results of simulation and user health, the results of shielding are widely discussed.

Owing to environmental and radiation health reasons, the source shield is one of the most important issues in the design of the detector system. And, because the distance from the source to the sample and the distance from the sample to the detector have a great impact on the intensity of the X-ray reaching the detector, it is necessary to use a material that can protect the source with a lesser thickness. In this case, lead and tungsten are two substances that can meet this important requirement. However, if lead is used as a source shield because it itself has secondary radiation, it would act as a noise. To remove lead noises, there should be a layer of copper and aluminum shields inside the parallel maker and the outer cover of lead. In this design, tungsten is a more appropriate option for shielding the source. The results of shielding using a tungsten shield

show that tungsten with a thickness of 0.25 cm for ^{57}Co source and with a thickness of about 0.15 cm for ^{241}Am source with 10 mci activation can be used as a suitable source shield.

The Response of the Optimized IXRF Device to Dust Elements

According to Table 2, the X-ray fluorescence energy of HR elements can be divided into two 5.41–17.48 keV and 74.98–98.43 keV intervals. The ^{241}Am source that emits 26.4(%) and 59.8(%) keV photons is suitable for the identification of the hazardous elements Cr, Co, Ni, Cu, Zn, Zr, Nb and Mo in the first interval and ^{57}Co , which emits the 122 keV photon, is suitable for the identification of the Pb and radioactive elements such as U and Th in the second interval. To calculate the response of the optimized IXRF device to dust HR elements, the AB1-87 dust sample that enters from neighbouring countries to the south and west of Iran was first chosen. Second, the HR elements of this sample were separately irradiated with two ^{241}Am and ^{57}Co sources. Figures 2 and 3 show the absorbed energy in CsI (TI) due to the K_{α} X-ray characteristic emitted by the irradiation of HR elements in the dust sample.

Figure 2 shows the hazardous elements (except Pb) are identifiable by the ^{241}Am source. Figure 3 shows that the Pb and radioactive elements are detectable by the ^{57}Co source. The Monte Carlo calculation of the pulse height created in the CsI (TI) detector due to the entry of the fluorescence radiation produced by the HR elements in the dust sample that are individually

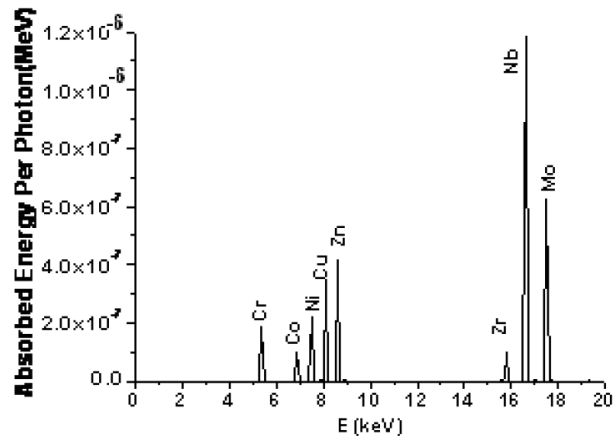


Figure 2: Absorbed energy spectrum of hazardous elements irradiated with ^{57}Co source.

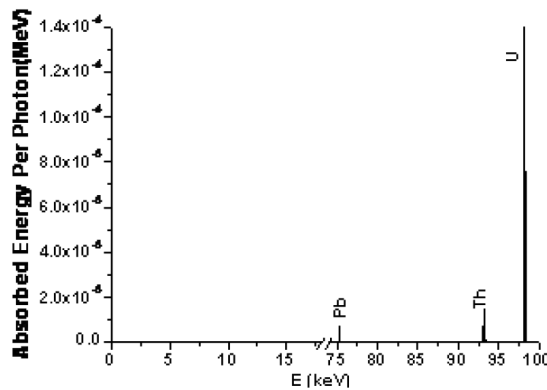


Figure 3: Absorbed energy spectrum of Pb and radioactive elements irradiated with ^{57}Co source.

Table 3: The K_α pulse height and Chi-Square in the calculation of HR element percentage by Am and Co source irradiation

Classification		$K_{\alpha}(keV)$							
		Pulse height in pure elements by		Pulse height in mixture by		Element		$(Exp - Obs)^2/Exp$	
						percent by			
	Element	Am	Co	Am	Co	Am	Co	by Am	by Co
Hazardous elements	Cr	5.46E-4	7.89E-5	9.86E-7	2.15E-7	0.0018	0.0027	2.00E-5	4.50E-5
	Co	1.24E-3	2.29E-4	2.72E-6	5.43E-7	0.0022	0.0024	2.00E-5	8.00E-5
	Ni	1.48E-3	2.61E-4	3.12E-6	6.06E-7	0.0021	0.0023	5.00E-5	4.50E-5
	Cu	1.12E-3	2.41E-4	2.52E-6	4.80E-7	0.0022	0.002	2.00E-5	2.45E-6
	Zn	2.23E-3	2.79E-4	5.28E-6	7.60E-7	0.0023	0.0027	4.50E-5	2.45E-5
	Zr	5.06E-3	6.34E-4	1.08E-5	1.54E-6	0.0021	0.0024	5.00E-5	8.00E-5
	Nb	5.57E-3	7.02E-4	7.18E-4	8.96E-5	0.13	0.127	2.65E-6	4.05E-2
	Mo	6.01E-3	7.64E-4	1.30E-3	1.66E-4	0.21	0.22	1.42E-3	2.80E-4
	Pb	-	3.91e-4	-	8.72E-6	-	0.0022	-	2.00E-6
Radioactive elements	Th	-	4.49e-3	-	9.86E-5	-	0.002	-	2.45E-5
	U	-	4.61e-3	-	1.54E-3	-	0.33	-	1.20E-5
Pearson Chi-Square: $\chi^2 = \sum((Exp - Obs)^2/Exp)$								2.52E-5	4.36E-2

irradiated with ^{241}Am and ^{57}Co sources are shown in the second and third columns of Table 3. The data from these columns can be used to calculate the percentage of the HR elements in the dust sample.

Calculating the Percentage of Elements Using Pulse Height

To calculate the percentage of elements, the dust sample must be irradiated by the ^{241}Am and ^{57}Co sources. The percentage of element can be calculated by dividing the pulse height of the element in the irradiated dust sample at each characteristic energy (K_α) (the fourth and fifth columns of Table 3) to the pulse height obtained from the pure element in the same characteristic energy (K_α) (the second column of Table 3).

In Table 3, the percentage of HR elements computed with an MCNPX simulation was compared with their reported values in the AB1-87 (Table 1) sample. The Pearson Chi-Square value to detect these elements using the IXRF device by ^{241}Am and ^{57}Co sources are obtained respectively 2.52×10^{-5} , 4.36×10^{-2} . According to the critical values of Chi-Square and the degrees of freedom, the p -value is <0.01 ; hence, the confidence level is more than 95%.

The Activity of ^{241}Am and ^{57}Co Sources to Identify HR Elements

The response of the CsI (TI) detector before the amplification of X-ray emitted from the sample is a

function of source activity as in Equation (1) (Wagner et al., 2001).

$$I = \frac{E}{W} \gamma_1 \gamma_2 \gamma_3 e k A \quad (1)$$

In Equation (1), I is the current entered into the preamplifier in the unit of Pico Ampere (pA), which must be in the range of 10–100 nA, the E is energy remaining in every range in the detector per source particle in electron volts (eV), the W is the energy required for production of an ion pair in the CsI(Tl) crystal (equal to 2.3 (eV)) (Wagner et al., 2001), γ_1 CsI(Tl) the scintillation crystal quantum efficiency (equal to 12%) (Knoll, 2010), γ_2 is the light guiding efficiency (equal to 80%) (Knoll, 2010), γ_3 is the photocathode efficiency in converting photons to electrons (equal to 25%) (Carter, 1980), e is the electron charge (1.6×10^{-19} C), k is detector multiplication factor (equal to 5.4×10^4) (Carter, 1980) and A is the activity of the source in units of Becquerel (Bq).

Assuming that the current entering the preamplifier was in the range of 10–100 nanoamperes, the calculation results in this research was based on Equation (1), and the simulation results demonstrated that 1.64 mCi and 19 γ μ ci activities were required for the sources of ^{241}Am and ^{57}Co in the one-source version to detect HR elements in dust respectively.

The Low of Detection (LOD) of IXRF Device

Usually, for any device, Low of Detection (LOD) should be calculated because of the radiation intensity of the background. The LOD is defined based on the standard error of the radiation intensity of the background. In case the background error (σ_B) and the pulse error are equal, the device error (σ) is $\sigma = (2\sigma_B)^{1/2}$. For a confidence level of 99%, the LOD will be equal to Equations (2) and (3) (Tiwari et al., 2005).

$$\begin{aligned} \text{LOD} &= C_{DL} = 3 \times (\text{deviation}) / (\text{slope of calibration}) \\ &= 3 \sigma_B / m \end{aligned} \quad (2)$$

$$\begin{aligned} \sigma_B &= (I_B)^{1/2}, m = I_A / C_A, I_A = A \times f 8 \\ \Rightarrow C_{DL} &= C_A \times 3 (I_B)^{1/2} / A \times f 8 \end{aligned} \quad (3)$$

where I_A , C_A , A , $f 8$, N_B and C_{DL} (LOD) respectively are the net intensity, the percentage of element in mixture, the source activity, the pulse height, the background counts in a given time T , the minimum detectable concentration of analyte. I_B is the background intensity (N_B/T) and $m = I_A/C_A$, is the slope of analyte count-concentration curve or net intensity per one percentage of element in a mixture.

To enable the IXRF device to measure an element with 10 ppm concentration, the LOD must be less than 10 ppm, for example, 5 ppm. In this case, according to Equation (3), the source activity is equal to Equation (4).

$$\begin{aligned} A &= 3 C_A (I_B)^{1/2} / C_{DL} \times f 8 \\ &= 30 (I_B)^{1/2} / 5 \times f 8 = 6 (I_B)^{1/2} / f 8 \end{aligned} \quad (4)$$

According to Table 3, the lowest pulse height for ^{241}Am source is reported as 9.86×10^{-7} . The experimental background radiation (I_B) of the 2"×2" crystal size CsI(Tl) detector with and without shield is 18.4 cps and 525 cps respectively. In this case, according to Equation (4), the required activities for non-shield and shield detectors are 3.75 mci and 0.70 mci, respectively.

In the non-shield CsI(Tl) detector case, the ^{241}Am source activity (1.64 mci) (calculated in previous Section) is less than the activity required to detect elements with 10 ppm LOD (3.75 mci). Therefore, in this case, the IXRF device is not able to measure the HR elements with a concentration of 10 ppm. If the CsI(Tl) detector has a shield, then the activity required to detect elements with 10 ppm LOD is 0.7 mci, which is less than the ^{241}Am source activity (1.64 mci), and the IXRF device is able to measure HR elements with a concentration of 10 ppm.

The practical and simulation results show that by shielding the CsI (Tl) detector with copper, aluminum and tungsten having a thickness of 1 mm, the background noise is reduced by more than 95%. As a result, by shielding the CsI (Tl) detector, the IXRF device (with 1.64 mci ^{241}Am source) is able to measure the HR elements at a concentration of 10 ppm.

According to Table 3, the lowest pulse height for heavy metals and ^{57}Co source is reported as 8.72E-5. In this case, according to Equation (4), the activity required for a non-shield and shield detector is 17.27 mci and 3.21 mci, respectively.

The calculated activity of ^{57}Co source in previous Sections is 19 μ ci. It is less than the activity required to detect elements with 10 ppm LOD with and without shield (3.21 mci and 17.27 mci respectively). Therefore, the IXRF device (with 19 μ ci ^{57}Co source) is not able to measure the HR elements having a concentration of 10 ppm.

Conclusions

In this research, the parameters of an IXRF device were optimized to accurately detect HR elements in dust. To evaluate the IXRF device performance, the MCNPX code was applied. This code has the ability to trace

gamma radiation and the characteristic X-rays of various elements. At first, the accuracy of the code in detecting each HR element was evaluated and confirmed using the two sources ^{241}Am (26.4 and 59.6 keV) and ^{57}Co (122 keV). The results showed that for the detection of hazardous elements, except Pb with 10 ppm, the LOD needed a ^{241}Am with 1.64 mci activity; the detection of Pb and radioactive elements, needed a ^{57}Co with 19 μCi activity. Simulation and practical results show that the optimized IXRF device is able to accurately detect HR elements in dust.

References

- Akkurt, I., Tekin, H.O. and A. Mesbahi (2015). Calculation of detection efficiency for the gamma detector using MCNPX. *Acta Physica Polonica A*, **128(2)**: 332-334.
- Bamford, S., Wegrzynek, D., Chinea-Cano, E. and A. Markowicz (2004). Application of X-ray fluorescence techniques for the determination of hazardous and essential trace elements in environmental and biological materials. *Nukleonika*, **49(3)**: 87-95.
- Bearden, J.A. and A.F. Burr (1967). Reevaluation of X-ray atomic energy levels. *Reviews of Modern Physics*, **39(1)**: 125.
- Briner, W. (2010). The toxicity of depleted uranium. *International Journal of Environmental Research and Public Health*, **7(1)**: 303-313.
- Carter, D.R. (1980). Photomultiplier Handbook: Theory, Design, Application. Lancaster (PA): Burle Industries, Inc.
- Coleman, H.W. and W.G. Steele (2009). Experimentation, validation, and uncertainty analysis for engineers. John Wiley & Sons.
- Genc, S., Zadeoglulari, Z., Fuss, S.H. and K. Genc (2012). The adverse effects of air pollution on the nervous system. *Journal of Toxicology*.
- Gondal, M.A., Seddigi, Z.S., Nasr, M.M. and B. Gondal (2010). Spectroscopic detection of health hazardous contaminants in lipstick using laser induced breakdown spectroscopy. *Journal of Hazardous Materials*, **175(1)**: 726-732.
- Greaves, E.D., Bernasconi, G., Wobrauschek, P. and C. Streli (1997). Direct total-reflection X-ray fluorescence trace element analysis of organic matrix materials with a semiempirical standard. *Spectrochimica Acta Part B: Atomic Spectroscopy*, **52(7)**: 923-933.
- Kampa, M. and E. Castanas (2008). Human health effects of air pollution. *Environmental Pollution*, **151(2)**: 362-367.
- Knoll, G.F. (2010). Radiation detection and measurement. John Wiley & Sons.
- Pirsaheb, M., Zinatizadeh, A., Khosravi, T., Atafar, Z. and S. Dezfulezhad (2014). Natural Airborne Dust and Heavy Metals: A Case Study for Kermanshah, Western Iran (2005–2011). *Iranian Journal of Public Health*, **43(4)**: 460.
- Plumejeaud, S., Reis, A.P., Tassistro, V., Patinha, C., Noack, Y. and T. Orsière (2016). Potentially harmful elements in house dust from Estarreja, Portugal: Characterization and genotoxicity of the bioaccessible fraction. *Environmental Geochemistry and Health*, **40(1)**: 127-144.
- Thompson, A., Attwood, D., Gullikson, E., Howells, M., Kim, K.J., Kirz, J., Kortright, J., Lindau, I., Pianetta, P., Robinson, A. and J. Scofield (2016). X-Ray Data Booklet (Lawrence Berkeley National Laboratory, Berkeley, CA, 2009). There is no corresponding record for this reference, pp.1-2.
- Tiwari, M.K., Singh, A.K. and K.J.S. Sawhney (2005). Sample preparation for evaluation of detection limits in X-ray fluorescence spectrometry. *Analytical Sciences*, **21(2)**: 143-147.
- Tonetti, C. and R. Innocenti (2009). Determination of heavy metals in textile materials by atomic absorption spectrometry: verification of the test method. *AUTEX Research Journal*, **9(2)**: 66-70.
- Verma, H.R. (2007). X-ray fluorescence (XRF) and particle-induced X-ray emission (PIXE). Atomic and Nuclear Analytical Methods: XRF, Mössbauer, XPS, NAA and B63Ion-Beam Spectroscopic Techniques, pp.1-90.
- Wagner, A., Tan, W.P., Chalut, K., Charity, R.J., Davin, B., Larochelle, Y., Lennek, M.D., Liu, T.X., Liu, X.D., Lynch, W.G. and A.M. Ramos (2001). Energy resolution and energy–light response of CsI (Tl) scintillators for charged particle detection. *Nuclear Instruments and Methods in Physics Research Section A: Accelerators, Spectrometers, Detectors and Associated Equipment*, **456(3)**: 290-299.
- Yu, K.N., Yeung, Z.L.L., Lee, L.Y.L., Stokes, M.J. and R.C.W. Kwok (2002). Determination of multi-element profiles of soil using energy dispersive X-ray fluorescence (EDXRF). *Applied Radiation and Isotopes*, **57(2)**: 279-284.
- Zaravandi, A., Carranza, E.J.M., Moore, F. and F. Rastmanesh (2011). Spatio-temporal occurrences and mineralogical–geochemical characteristics of airborne dusts in Khuzestan Province (southwestern Iran). *Journal of Geochemical Exploration*, **111(3)**: 138-151.
- Župunski, L., Spasić-Jokić, V., Trobok, M. and V. Gordanić (2010). Cancer risk assessment after exposure from natural radionuclides in soil using Monte Carlo techniques. *Environmental Science and Pollution Research*, **17(9)**: 1574-1580.

Contents

<i>Editorial</i>	i
❑ <i>Snapshots</i>	ii
Expander-based Atmospheric Water Harvesting in the Tropics	
<i>Alison Subiantoro</i>	1
Assessment of Runoff and Sediment Yield in the Tilaya Reservoir, India Using SWAT Model	
<i>Debobroto Dutta, Rajib Das and Asis Mazumdar</i>	9
Variation in the Chemical Status of Water and Soil Sediments along Saiwa Swamp Ecosystem, Trans Nzoia County, Kenya	
<i>W.S.K. Ruto, J.I. Kinyamario, J.I. Kanya and N.K. Ng'etich</i>	19
An Optimization Model Using the Standard Deviation Method and Multiple Decision Making Statistics in Water Treatment Plants in Northeastern India	
<i>Sudipa Choudhury, Mrinmoy Majumder and Apu Kumar Saha</i>	27
Predicting Water Availability of the Regulated Mekong River Basin Using Satellite Observations and a Physical Model	
<i>Faisal Hossain, Safat Sikder, Nishan Biswas, Matthew Bonnema, Hyongki Lee, N.D. Luong, N.H. Hiep, Bui Du Duong and Duc Long</i>	39
Ground Water Quality Assessment through Index Method and Health Status: A Case Study of Firozabad City (India)	
<i>Nikhat Bano</i>	49
A Case Study on Sustainable Development in Coal India Limited	
<i>S. Raghavendra, S. Pardhasaradhi and Swetha Suram</i>	57
Framework for Assessing Efficient Water Consumption Attributes and Their Relative Importance in Office Complexes	
<i>Gaurav Chandra, Manjari Chakraborty and A.K. Sinha</i>	65
Irrigation Water Quality Based on Hydro Chemical Analysis of Ganga-Sone Divide Region of Bihar	
<i>Priti Kumari</i>	75
❑ <i>Short Notes</i>	
The Impact of Ecotourism in Taman Negara National Park, Malaysia: Tourist Perception on Its Environmental Issues	
<i>Mohd Sayuti Hassan and Sharifah Nurlaili Farhana Syed Azhar</i>	85
Fluoride Contamination in the Ground Water of Two Villages of Visakhapatnam Industrial Area	
<i>G.V.S.R. Pavan Kumar, Yerra Bharath and M. Komal Avinash</i>	91
<i>Environment News Futures</i>	103